

# Triethylsilanol: Molecular Conformations and Role of the Hydrogen-Bonding Oligomerization in Its Vibrational Spectra

Manuel Montejo, Francisco Partal Ureña, Fernando Márquez, and Juan Jesús López González\*

Physical and Analytical Chemistry Department, University of Jaén, Campus Las Lagunillas, E-23071 Jaén, Spain

Received: October 23, 2007; In Final Form: November 22, 2007

We report a theoretical study of the molecular structure of the triethylsilanol molecule and a thorough conformational analysis of the species following the Boltzmann's distribution law. The vibrational spectra of the title molecule have been assigned by means of the combined use of experimental data obtained from IR and Raman spectra and theoretical DFT calculations with the subsequent implementation of the SQMFF methodology. The role of hydrogen bonding in the shifting of the vibrational bands of the silanol group in the spectra of the liquid phase is discussed using a model of triethylsilanol dimer.

## Introduction

Silanols are known to be intermediates in the sol–gel processes of organosilicon compounds to obtain oxidic materials of industrial interest such as fibers, glasses, monodispersing powders, etc.<sup>1</sup> Two different types of reactions take place during the sol–gel processes of organosilicon compounds; hence, in the first stage, the precursors (silicon alkoxides) hydrolyze giving silanols that, in the second stage, condense into oxidic networks.<sup>1</sup> Given that the mechanism and kinetics of the reaction strongly influence the properties of the final products, the monitoring of these processes is an important issue of study and different experimental techniques are nowadays being used for this task. Among them, IR and Raman spectroscopies have been extensively used.<sup>2</sup> Specifically, the appearance and disappearance during the two stages of the process of the vibrational bands of the silanol group could be indicative of the reaction progress and its mechanism. Hence, the study of the vibrational spectra of molecular systems containing the silanol group could be of interest.

The simplest model containing the SiOH group, the silanol molecule, H<sub>3</sub>SiOH, has been theoretically studied in many works,<sup>3</sup> including the effect of hydrogen-bonding oligomerization in its vibrational spectrum.<sup>4</sup> Additionally, systems with bulky alkyl substituents, which are stable, have been used to obtain experimental information about the silanol group.<sup>5</sup> Nevertheless, the assignment of the SiOH group frequencies has been controversial in this type of molecule given that these normal modes are usually mixed with vibrations of the alkyl moiety. For that reason, use of theoretical methods for calculation of the vibrational spectra of these compounds and, specifically, implementation of the SQMFF (scaled quantum mechanics force field) methodology<sup>6</sup> can be helpful for a better understanding of the experimental features.

Previous works of our group have dealt with the study of the vibrational spectra of several trialkylsilyl derivatives.<sup>7</sup> These works have allowed us to obtain sets of scaling factors useful for estimation of the vibrational spectra of the alkyl moiety (i.e., methyl and ethyl groups) of silyl derivatives.

In order to continue our study, the vibrational spectra of triethylsilanol have been studied in the present work aiming to obtain spectral information on the silanol group vibrations. This species has been selected for two main reasons: it is relatively stable to processes of self-condensation, which facilitates obtaining experimental data, and its moderate molecular size, which makes it appropriate for theoretical studies.

There are several previous works concerning the vibrational spectra of triethylsilanol. During the 1950s, Ryskin et al.<sup>8</sup> recorded the IR and Raman spectra of several ethylsilyl species (including triethylsilanol) and their deuterated derivatives in a series of works in which the first attempts of assignment of the vibrational spectra for these species were reported. Later, Kriegsmann et al.<sup>9</sup> recorded the IR and Raman spectra of several alkyl and aryl silanols in liquid phase and solved in CS<sub>2</sub> and CCl<sub>4</sub>. In addition to the vibrational assignment, these studies were focused on analysis of the effect of the alkyl chain, the concentration of the corresponding silanol, and the nature of the solvent on hydrogen bonding by means of analysis of the displacement of the OH vibrations.

More recently, Carteret<sup>10</sup> thoroughly revised the characteristic vibrations of the silanol group present in several alkylsilanols and models of silica surfaces, combining both experimental information and DFT calculations.

Despite the number of previous papers dealing with the vibrational spectra of triethylsilanol, its molecular structure has been studied neither experimentally nor theoretically until now. For this reason, our first task is to study theoretically the molecular and electronic structure of triethylsilanol, including a thorough conformational analysis based on the Boltzmann populations. Our second goal is to perform a complete assignment of the vibrational spectra of triethylsilanol combining experiment and theory on the basis of DFT calculations and implementation of the SQMFF methodology.<sup>6</sup> This scheme will allow us to obtain scale factors for the SiOH group that may be used for theoretical estimation of the position of its characteristic vibrational bands in the intermediate species generated during the sol–gel processes. Finally, we aim to discuss the hydrogen bonding in such species by analyzing the experimental shifts of the vibrational bands of the SiOH group in the vibrational

\* To whom correspondence should be addressed. Phone: +34953212754. Fax: +34953212940. E-mail: jjlopez@ujaen.es.

spectra of the liquid phase using for this task a theoretical triethylsilanol dimer as a model for computational calculations.

### Experimental Details

Triethylsilanol samples ( $\geq 98\%$ ) were purchased from Sigma-Aldrich. IR spectra of the liquid and gas phases were recorded in the 390–4000  $\text{cm}^{-1}$  range using a FT-IR Bruker Vector 22 spectrophotometer, equipped with a Globar source and a DTGS detector, using standard cells for liquid and gas (10 cm path length) with CsI windows. The spectra were obtained with a resolution of 1  $\text{cm}^{-1}$ .

The Raman spectrum of the liquid phase was recorded with a Bruker RF100/S FT-Raman spectrometer, equipped with a Nd:YAG laser (excitation line 1064 nm, 600 mW of laser power) and a cooled Ge detector at liquid nitrogen temperature, using a standard liquid cell. The spectra were again recorded with a resolution of 1  $\text{cm}^{-1}$ .

### Computational Details

All molecular orbital and DFT calculations reported were performed using the Gaussian 03 program package.<sup>11</sup> Geometry optimizations and frequency calculations for the different conformers were carried out using the MP2 and B3LYP methods in conjunction with two basis sets, namely, Pople's standard split 6-31G\* basis set and the augmented correlation-consistent double- $\zeta$  basis set of Dunning (aug-cc-pVDZ). Each stationary point obtained was characterized by the vibrational frequencies computation at the same level of theory.

The force fields obtained in Cartesian coordinates at the B3LYP/6-31G\* level were transformed into natural valence coordinates in order to implement the SQMFF methodology.<sup>6</sup> Then, we transferred to triethylsilanol the scale factors obtained in a previous work for the triethylsilyl moiety.<sup>7a</sup> The scale factors associated with the force constants of the natural coordinates defining the vibrations of the  $-\text{SiOH}$  group were refined, taking 1.000 as a starting value, by a root-mean-squares fitting of the theoretical frequencies to those observed experimentally. The lack of experimental data prevented refinement of the scale factor associated with the torsion of the SiO bond.

The force field transformations into natural valence coordinates, refinement of the scale factors, and normal-mode analysis were performed using the MOLVIB program.<sup>12</sup>

Natural bond orbital (NBO)<sup>13</sup> calculations were carried out using the NBO 3.1 program<sup>14</sup> as implemented in Gaussian 03.

### Results and Discussion

**Theoretical Conformational Analysis.** The search for the conformers of triethylsilanol was performed by rotating the three ethyl groups that can adopt either gauche (g) or anti (a) orientations with respect to the Si–O bond (as stated in ref 7a, which concerns two related triethylsilyl derivatives, namely, triethylchloro- and triethylbromosilane, TECS and TEBS, respectively). The presence of eclipsed conformations was discounted. The  $-\text{OH}$  group adopts an anti position with respect to the Si–C bonds. Twelve different conformers have been identified as minima at the potential-energy surface of triethylsilanol.

The relative differences (in  $\text{kJ mol}^{-1}$ ) between the Gibbs free energies ( $\Delta G$ ) for all 12 conformers of triethylsilanol calculated using MP2 and B3LYP methods with 6-31G\* and aug-cc-pVDZ basis sets are reported in Table 1.

Theoretical calculations yield very low energy differences (ca. 1  $\text{kJ mol}^{-1}$ ) among six conformers, namely, I, III, IV, VII,

**TABLE 1: Relative Gibbs Free Energies ( $\Delta G$ , in  $\text{kJ mol}^{-1}$ ) of the 12 Conformers Defined for Triethylsilanol Calculated with the B3LYP and MP2 Methods and the 6-31G\* and aug-cc-pVDZ Basis Sets**

conformer	B3LYP		MP2	
	6-31G*	aug-cc-pVDZ	6-31G*	aug-cc-pVDZ
I	0.00	0.00	0.45	1.27
II	3.57	3.03	5.04	8.52
III	0.54	0.05	0.80	0.70
IV	0.10	0.28	0.00	0.00
V	4.21	3.36	3.46	3.39
VI	3.42	3.48	3.72	3.15
VII	0.87	0.75	1.13	0.79
VIII	0.75	0.63	1.28	1.12
IX	0.16	0.51	1.11	1.12
X	0.76	1.44	4.89	5.19
XI	1.85	2.59	5.26	5.48
XII	2.17	1.27	5.04	5.42

**TABLE 2: Theoretical Boltzmann Populations (%) for Each of the 12 Conformers of Triethylsilanol at 298 K**

conformer	B3LYP		MP2	
	6-31G*	aug-cc-pVDZ	6-31G*	aug-cc-pVDZ
I	14.2	14.3	16.5	12.3
II	3.3	4.2	2.6	0.7
III	5.7	7.0	7.2	7.7
IV	13.6	12.8	19.8	20.5
V	2.6	3.7	4.9	5.2
VI	3.6	3.5	4.4	5.7
VII	10.0	10.5	12.6	14.9
VIII	10.5	11.0	11.8	13.0
IX	13.3	11.6	12.7	13.0
X	10.5	8.0	2.7	2.5
XI	6.7	5.0	2.4	2.2
XII	5.9	8.5	2.6	2.3

VIII, and IX. These differences are slightly higher (up to 5  $\text{kJ mol}^{-1}$ ) for the remaining conformers, i.e., II, V, VI, X, XI, and XII. However, B3LYP and MP2 methods calculate different conformers to be the global minimum of the system (those called I and IV, respectively).

We used the Boltzmann distribution equation in order to obtain information about the relative abundance of each conformer in the gas phase and take into account the relative multiplicities of the conformers based on their symmetry.

At both B3LYP and MP2 levels only five conformers, namely, I, IV, VII, VIII, and IX, were found to have populations above 10% as shown in Table 2. The sum of their populations amounts to ca. 70% of the sample composition in the gas phase. Populations for conformers II, III, V, VI, X, XI, and XII (Figure 1S of the Supporting Information) are sensibly smaller.

The molecular representation and atom numbering of the five main conformers found for triethylsilanol are shown in Figure 1. Remarkably, all conformers are related with the main conformers found for the triethylhalo derivatives previously studied.<sup>7a</sup> Conformers VII, VIII, and IX (all of  $C_1$  symmetry) are related with the main calculated conformer in TECS and TEBS that has also  $C_1$  symmetry ( $ag+g+$ ), with the  $-\text{OH}$  group in the anti position with respect to the three ethyl groups. Moreover, conformer IV ( $C_1$  symmetry) is related with the  $C_s$  ( $ag-g+$ ) conformer of TECS and TEBS, with the  $-\text{OH}$  group oriented in the anti position with respect to the SiC bond of one of the gauche ethyl groups. Finally, conformer I ( $C_1$ ) is related to the  $C_3$  ( $g+g+g+$ ) conformer of TECS and TEBS.

**Theoretical Molecular Structure.** To the best of our knowledge, this is the first report of the molecular structure of the title compound from either a theoretical or an experimental point of view. The main geometrical parameters obtained

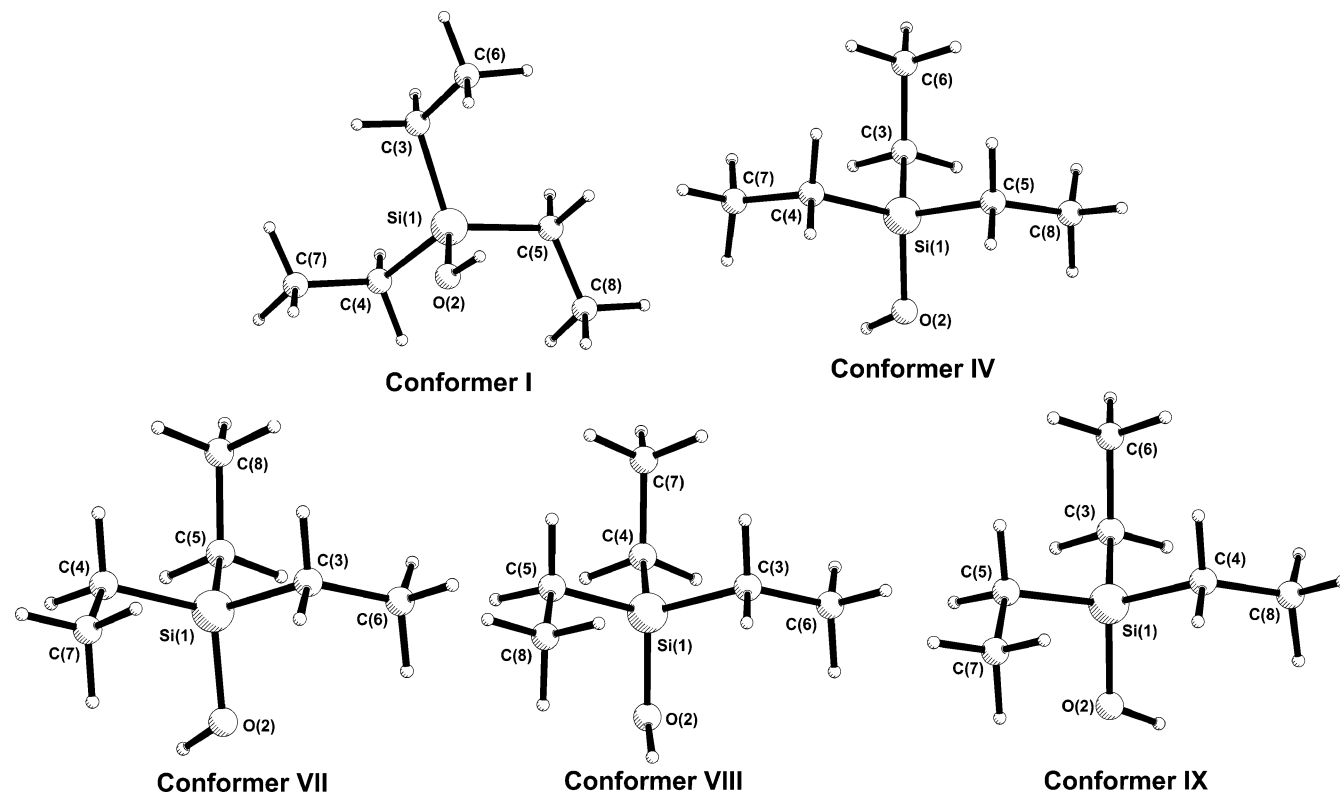


Figure 1. Molecular representation and atom numbering of the five main conformers of triethylsilanol.

TABLE 3: Comparison of the Main Geometrical Parameters Calculated for the Five Main Conformers of Triethylsilanol at the MP2/aug-cc-pVDZ Level (Distances in Angstroms, Angles in Degrees)

parameters	MP2/aug-cc-pVDZ				
	I	IV	VII	VIII	IX
$r_{\text{SiO}}$	1.718	1.716	1.717	1.716	1.716
$r_{\text{OH}}$	0.966	0.966	0.966	0.966	0.966
$r_{\text{SiC}_3}$	1.895	1.896	1.887	1.896	1.896
$r_{\text{SiC}_4}$	1.886	1.894	1.895	1.886	1.896
$r_{\text{SiC}_5}$	1.895	1.887	1.894	1.895	1.886
$r_{\text{C}_3\text{C}_6}$	1.542	1.543	1.542	1.542	1.542
$r_{\text{C}_4\text{C}_7}$	1.542	1.542	1.543	1.543	1.543
$r_{\text{C}_5\text{C}_8}$	1.542	1.542	1.542	1.542	1.543
$\angle_{\text{SiOH}}$	115.4	115.3	115.3	115.4	115.5
$\angle_{\text{C}_3\text{SiO}}$	109.7	109.9	103.4	109.8	110.1
$\angle_{\text{C}_4\text{SiO}}$	103.3	110.5	110.6	104.3	110.5
$\angle_{\text{C}_5\text{SiO}}$	110.1	104.2	110.3	110.6	103.8
$\angle_{\text{C}_3\text{SiC}_4}$	111.8	109.5	110.8	110.7	109.2
$\angle_{\text{C}_4\text{SiC}_5}$	111.7	111.4	110.3	111.5	111.9
$\angle_{\text{C}_5\text{SiC}_3}$	110.0	111.1	111.3	109.8	111.3
$\angle_{\text{C}_6\text{C}_3\text{Si}}$	113.4	112.6	113.2	113.2	113.5
$\angle_{\text{C}_7\text{C}_4\text{Si}}$	113.4	113.5	113.0	113.1	113.1
$\angle_{\text{C}_8\text{C}_5\text{Si}}$	113.8	113.4	113.4	113.7	113.4

theoretically at the MP2/aug-cc-pVDZ level for the five main conformers of triethylsilanol are reported in Table 3. The reliability of the theoretical structures calculated with this method for this type of molecule was proven in ref 7a.

We found low differences among the calculated geometrical parameters when comparing the results for the different conformers. However, within each conformer the calculated SiC bond distances and CSiO angles are affected by their relative position with respect to the OH group. As a result, the SiC bond in the anti position with respect to the OH group is predicted to be ca. 0.010 Å shorter than the other two SiC bond lengths. Additionally, the CSiO bond angles involving the shorter SiC bond are calculated to be ca. 6° smaller than the other two.

TABLE 4: NBO Electronic Populations (in au) of the Lone Pair Orbitals of the Oxygen Atom and the  $\sigma$  and  $\sigma^*$  Orbitals of the SiC Bonds in Triethylsilanol Calculated at the MP2/aug-cc-pVDZ Level

orbital	electronic population (au)				
	I	IV	VII	VIII	IX
LP(1)	1.9779	1.9781	1.9779	1.9779	1.9776
LP(2)	1.9588	1.9583	1.9585	1.9584	1.9589
$\sigma_{\text{SiC}_3}$	1.9618	1.9603	1.9604	1.9609	1.9606
$\sigma_{\text{SiC}_4}$	1.9612	1.9617	1.9613	1.9605	1.9614
$\sigma_{\text{SiC}_5}$	1.9614	1.9615	1.9618	1.9614	1.9612
$\sigma^*_{\text{SiC}_3}$	0.0479	0.0494	0.0404	0.0514	0.0525
$\sigma^*_{\text{SiC}_4}$	0.0366	0.0499	0.0473	0.0365	0.0476
$\sigma^*_{\text{SiC}_5}$	0.0484	0.0375	0.0491	0.0493	0.0368

The influence of the hyperconjugative effects in the calculated geometries was analyzed with the help of NBO analysis carried out for their respective electronic structures.

In Table 4 the electron populations of the lone pairs of the oxygen atoms and the  $\sigma$  and  $\sigma^*$  orbitals of the SiC bond are reported. The occupation of the antibonding orbital of the SiC bond placed in the anti position with respect to the OH bond (see Figure 1) is appreciably lower than in the other two SiC bonds. Since high populations in the antibonding orbitals lead to a weakening and lengthening of the bonds, these mentioned differences may explain the variation in the calculated equilibrium distances for the same type of bond within one molecule.

As shown in Table 5 for the five conformers the interaction between the LP(2) of the oxygen atom and the  $\sigma^*_{\text{SiC}}$  orbitals was found to be weaker in the case of the shorter SiC bond. Moreover, the presence of a stabilizing interaction between the  $\sigma^*$  orbital of the OH bond and the  $\sigma$  orbital of the SiC bond in the anti position may explain the contraction of this CSiO angle.

**Vibrational Study.** The IR spectra of the gas and liquid phases and the Raman spectrum of the liquid phase of triethylsilanol are shown in Figure 2.

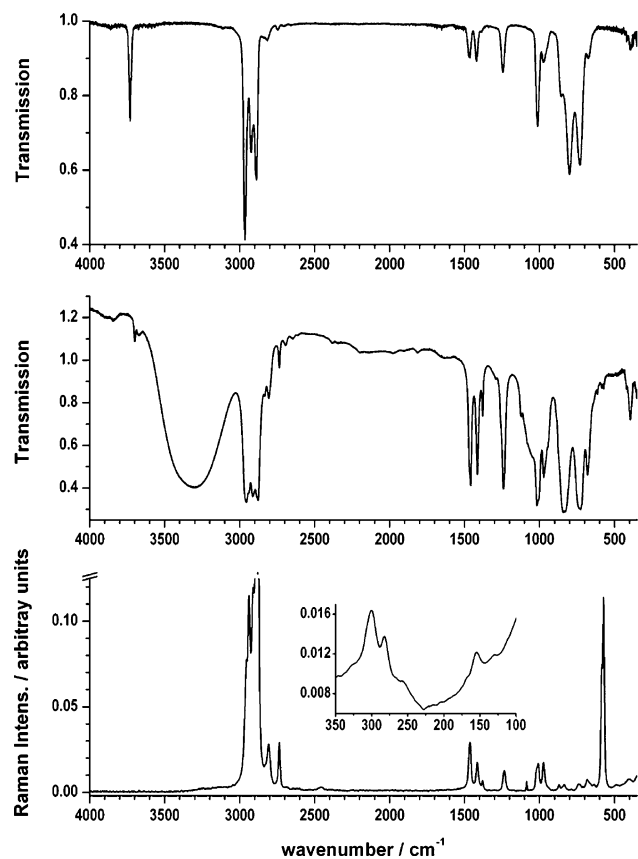


**Figure 2.** IR spectra of the gas (up) and liquid (middle) phases and Raman spectrum of the liquid phase (bottom) of triethylsilanol.

**TABLE 5: Magnitude (in  $\text{kJ mol}^{-1}$ ) of the Interactions between the Two Lone Pair Orbitals of the Oxygen Atom and the  $\sigma^*$  Orbitals of the SiC Bonds and between the Bonding SiC Orbital and the Antibonding OH Orbital in Triethylsilanol Calculated at the MP2/aug-cc-pVDZ Level**

interaction	$E^{(2)}$ ( $\text{kJ mol}^{-1}$ )				
	I	IV	VII	VIII	IX
LP(1) $\rightarrow \sigma^*\text{SiC}_3$	7.32	14.43	15.77	9.16	6.57
LP(1) $\rightarrow \sigma^*\text{SiC}_4$	16.28	2.22	10.84	16.15	9.04
LP(1) $\rightarrow \sigma^*\text{SiC}_5$	7.45	13.85	4.73	6.19	16.15
LP(2) $\rightarrow \sigma^*\text{SiC}_3$	36.07	22.01		32.89	38.74
LP(2) $\rightarrow \sigma^*\text{SiC}_4$		47.36	31.25		34.52
LP(2) $\rightarrow \sigma^*\text{SiC}_5$	36.90	4.60	42.09	40.33	
$\sigma\text{SiC}_3 \rightarrow \sigma^*\text{OH}$			6.36		
$\sigma\text{SiC}_4 \rightarrow \sigma^*\text{OH}$	6.32			6.49	
$\sigma\text{SiC}_5 \rightarrow \sigma^*\text{OH}$		5.90			6.28

The widely used B3LYP/6-31G\* method, whose performance for this sort of molecule has been previously discussed,<sup>7</sup> was chosen for vibrational analysis. Thus, the scale factors for the triethylsilyl moiety obtained with this method in a previous work<sup>7a</sup> were transferred to the five main conformers of triethylsilanol.

Additionally, the normal-mode frequencies of the SiOH group predicted theoretically for conformer I were fitted to the bands observed in the IR spectrum of the gas phase by means of a root-mean-squares procedure following the SQMFF methodology.<sup>6</sup> The normal modes characteristic of the silanol group are as follows: the torsion around the SiO bond, the bending of the SiOH bond, and the stretching of the SiO and OH bonds.

The scale factors obtained for the vibrations of the silanol group, reported in Table 6, were later transferred to conformers IV, VII, VIII, and IX. The scaled frequencies for the five main conformers of triethylsilanol, the experimental frequencies of

**TABLE 6: Sets of Averaged Scale Factors for the Triethyl Moiety Transferred to Triethylsilanol (Taken From Ref 7a)<sup>a</sup>**

scale factor	B3LYP/6-31G*
SiC st.	1.026
CC st.	0.949
CH st. ( $=\text{CH}_2$ )	0.905
CH st. ( $\text{CH}_3$ )	0.897
$\text{CH}_2$ sc.	0.914
$\text{SiC}_3$ sc.	1.064
$\text{CH}_2$ rock.	0.949
$\text{CH}_2$ wag.	0.936
$\text{CH}_2$ tw.	0.938
Sym. $\text{CH}_3$ def.	0.924
asym. $\text{CH}_3$ def.	0.899
$\text{CH}_3$ rock.	0.965
sym. $\text{SiC}_3$ def.	0.768
asym. $\text{SiC}_3$ def.	0.965
$\text{SiC}_3$ rock.	0.736
SiC torsion	1.000
CC torsion	0.905
<b>OH st.</b>	<b>0.961</b>
<b>SiO st.</b>	<b>0.916</b>
<b>SiOH def.</b>	<b>0.914</b>
<b>SiO torsion</b>	<b>1.000</b>

<sup>a</sup> At the end of the table and in bold, the scale factors for the silanol group vibrations obtained in the present work are also reported.

the bands associated to fundamentals with their relative intensities, the proposed vibrational assignment, and the main terms of the PED are reported in Table 7.

Following this scheme we can explain experimental features observed in the IR spectrum of the gas phase in accordance with previous authors.<sup>9</sup> Specifically, the normal modes associated with the silanol group were assigned in accordance with previous works<sup>8-10</sup> as follows: the band appearing at  $3730 \text{ cm}^{-1}$  is assigned to the stretching of the isolated OH bond, the band appearing at  $855 \text{ cm}^{-1}$  is assigned to the SiOH valence angle deformation, and the band observed at  $801 \text{ cm}^{-1}$  is assigned to the SiO bond stretching. The torsion of the SiO bond, calculated at ca.  $200 \text{ cm}^{-1}$  with the B3LYP/6-31G\* method, is not observed.

Moreover, the experimental profile of the IR spectrum of the gas phase is also in reasonable good agreement with the conformationally averaged IR spectrum calculated with the B3LYP/aug-cc-pVDZ method (Figure 2S) that we plotted taking into account the weighted contributions according to their Boltzmann populations of the 12 conformers of triethylsilanol.

In contrast with the IR spectrum of the gas phase, the vibrational spectra of the liquid phase (IR and Raman) present a more complex band shape (Figure 2) due to formation of hydrogen bonds. Despite this, the normal modes of the triethylsilyl moiety are accurately reproduced (Table 7). Moreover, taking into consideration more than one conformer, we assigned some spectral features observed only in the spectra of the liquid phase. This is the case of the SiC stretching and of some low-frequency vibrations (see Table 7).

Nevertheless, the vibrational bands involving the SiOH group, which will be discussed below, appear considerably shifted due to the effect of hydrogen bonding. In order to explain the experimental features observed and analyze the influence of hydrogen bonding on the vibrational band positions of triethylsilanol, a dimer, designed from two units of the conformer I, was optimized at the B3LYP/aug-cc-pVDZ level (Figure 3). The strength of the hydrogen bonding in the dimer is demonstrated using the NBO methodology, which detected two stabilizing interactions ( $E^{(2)} = 32.34$  and  $15.40 \text{ kJ mol}^{-1}$ , respectively) from the lone pairs of the donor oxygen to the

**TABLE 7. Experimentally Observed Bands (with Relative Intensities) and Scaled Frequencies (in  $\text{cm}^{-1}$ ) at the B3LYP/6-31G\* Level for the Five Main Conformers of Triethylsilanol, Including the Proposed Assignments and the Main Terms of the PED for Each Mode (All the Normal Modes Have A Symmetry)**

scaled B3LYP/6-31G*					experimental <sup>d</sup>			assignment <sup>b,c</sup>
I	IV	VII	VIII	IX	IR gas	IR liquid	Raman liquid	
43	39	43	43	39				$\tau\text{SiC}$
58	51	59	53	54				
64	79	68	69	67				
114	100	104	107	104				$\delta^{\text{as}}\text{SiC}_3$ (scSiC <sub>3</sub> )
118	153	134	133	133			154 vw	
144	133	141	140	144				$\delta^{\text{s}}\text{SiC}_3$
169	162	167	170	168				$\rho\text{SiC}_3 + \tau\text{CC}$
175		181	176	173				
	175							$\tau\text{SiO}$ ( $\tau\text{CC}$ )
197	196	197	197	192				
227	221	221	220	219				$\tau\text{CC} + \text{scSiC}_3$
243	238	242	246	244				$\tau\text{CC} + \rho\text{SiC}_3$
253	262	255	253	251				
270							281 vw	$\delta^{\text{s}}\text{SiC}_3 + \tau\text{CC}$
	296	298	292	297			300 vw	scSiC <sub>3</sub> + $\delta^{\text{as}}\text{SiC}_3$
	327	330	334	331				scSiC <sub>3</sub> + $\delta^{\text{s}}\text{SiC}_3$
	369							scSiC <sub>3</sub>
375		392	394	387	392 w	394 m	397 vw	
384		562	562	561		571 w	572 s	$\nu\text{SiC}$
561						583 w	584 m, sh	
	573					614 vw		$\tau\text{SiO}$ (oligomers) <sup>d</sup>
640	631	635	630	634			636 vw	$\rho\text{CH}_2$ ( $\nu\text{SiC}$ )
648	669	664	665	663				
686	679	675	676	678	674 w	679 s	683 vw	
713		717	713	721			711 vw	$\nu\text{SiC}$
	718							$\rho\text{CH}_2$
725	732	734	740	736	734 s	727 vs	740 vw	$\nu\text{SiC} + \rho\text{CH}_2$
799	805	806	807	805	801 s			$\nu\text{SiO}$ ( $\delta\text{SiOH}$ )
						826 vs	835 br,w	$\nu\text{SiO}$ (oligomers) <sup>d</sup>
						841 vs		
855	855	852	856	854	855 m, sh		870 vw	$\delta\text{SiOH}$ ( $\nu\text{SiO}$ )
								$\delta\text{SiOH}$ (oligomers) <sup>c</sup>
941	933	938	938	938		944 w, sh		twCH <sub>2</sub> + $\rho\text{CH}_3$
949		947	941	944				
	950							$\rho\text{CH}_3 + \text{waCH}_2$
	958							
953		959	960	959				$\rho\text{CH}_3 + \text{waCH}_2 + \nu\text{CC}$
	965							twCH <sub>2</sub> + $\rho\text{CH}_3 + \nu\text{CC}$
	968							
967		966	966	964				$\nu\text{CC} + \rho\text{CH}_3$
970	972	969	969	970				
975		976	974	976	974 w	971 s	974 w	$\nu\text{CC} + \text{twCH}_2 + \rho\text{CH}_3$
1009	1008	1012	1010	1011		1005 vs	1009 w	$\nu\text{CC} + \rho\text{CH}_3$
	1014	1019	1018	1015	1012 s	1017 vs	1017 w, sh	
1024								
1027	1030	1027	1025	1026				$\delta\text{SiOH}$ (oligomers) <sup>d</sup>
						1121 s		
						1081 sh	1086 w	
						1046 sh		
1240	1239	1239	1238	1240	1244 m	1240 s	1234 w	twCH <sub>2</sub> + $\rho\text{CH}_3$
1242	1241	1243	1240	1242				
1249	1246	1245	1245	1246				
1253	1256	1256	1255	1256				waCH <sub>2</sub>
1260	1259	1258	1257	1257				
1263	1262	1263	1263	1263				
1385	1383	1384	1384	1384				$\delta^{\text{s}}\text{CH}_3$
1385	1385	1386	1386	1385				
1386	1386	1386	1388	1387				
1420	1418	1421	1421	1420	1419 m	1415 s	1416 w	sc CH <sub>2</sub>
1422	1425	1423	1424	1423				
1424	1427	1426	1427	1426				
1456	1455	1457	1456	1455	1468 m	1459 vs	1463 w	$\delta^{\text{as}}\text{CH}_3$
1458	1457	1458	1457	1458				
1459	1460	1459	1459	1459				
1461	1461	1461	1460	1462				
1462	1463	1462	1464	1463				
1464	1464	1464	1464	1464				
2866	2872	2865	2868	2671	2887 vs	28 77 vs	879 vs, p	$\nu^{\text{s}}\text{CH}_2$
2874	2874	2869	2874	2875				
2876	2877	2877	2887	2876				
2874	2875	2879	2875	2874				$\nu^{\text{s}}\text{CH}_3$
2881	2879	2880	2878	2879				
2882	2881	2881	2880	2881				
2897	2907	2897	2898	2906	2923 vs	2912 vs	2910 vs, p	$\nu^{\text{s}}\text{CH}_2$
2910	2909	2908	2908	2909				
2912	2911	2912	2917	2911				
2930	2931	2934	2931	2930				$\nu^{\text{as}}\text{CH}_3$
2935	2934	2935	2935	2934				
2937	2935	2936	2936	2935				
2940	2938	2944	2939	2938		2943 sh	2937 vs, p	
2949	2943	2949	2942	2943				
2956	2955	2955	2948	2956	2964 vs	2954 vs	2952 sh, p	$\nu\text{OH}$ (network) <sup>d</sup>
						3308 vs, br		$\nu\text{OH}$ (oligomers) <sup>d</sup>
						3671 vw		
						3700 vw		
3730	3732	3729	3729	3731	3730 s			$\nu\text{OH}$ (isolated) <sup>d</sup>

<sup>a</sup> Abbreviations: vs = very strong, s = strong, m = medium, w = weak, vw = very weak, sh = shoulder, br = broad, p = polarized, dp = depolarized. <sup>b</sup> Only shown contributions higher than 10%. <sup>c</sup> Symbols used:  $\nu$  = stretching,  $\delta$  = deformation,  $\rho$  = rocking,  $\tau$  = torsion, sc = scissoring, tw = twisting, wa = wagging. Superscripts "s" and "as" denote symmetric and asymmetric motions. <sup>d</sup> See text for explanation.

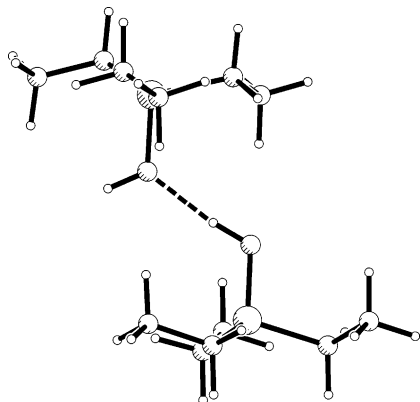


**Figure 3.** Molecular representation of the dimer of triethylsilanol modeled from two units of conformer I.

antibonding  $\sigma^*OH$  orbital of the acceptor unit. The optimized Cartesian coordinates of the dimer and the vibrational frequencies calculated at the above-mentioned level are collected in Tables 1S and 2S of the Supporting Information.

As shown in Table 7, the calculated frequency for the torsion around the SiO bond in the triethylsilanol monomer, at ca.  $195\text{ cm}^{-1}$ , has no correspondence with any of the observed bands in the vibrational spectra. As for the dimer, the torsional motion suffers a blue shift of ca.  $400\text{ cm}^{-1}$ , being calculated at  $609\text{ cm}^{-1}$ . A very weak band at  $614\text{ cm}^{-1}$  is also observed in the IR spectrum of the liquid phase, as shown in Table 7, which is not present in the IR spectrum of the gas phase. Our assignment of this band to  $\tau SiO$  is also supported by the results of Ignatyev et al.<sup>5e</sup> that predicted a blue shift for this frequency in the trimethylsilanol case. Additionally, in a previous work, Ignatyev et al.<sup>4</sup> reported that the out-of-plane deformation of the  $H\cdots OH$  angle in the silanol molecule dimer appeared at  $620\text{ cm}^{-1}$ . This result is also in accordance with our observations in triethylsilanol.

The stretching mode of the SiO bond appears as a strong band at  $801\text{ cm}^{-1}$  in the IR spectrum of the gas phase. Nevertheless, in the vibrational spectra of the liquid phase, this band is considerably shifted. Previous authors (ref 10 and references therein) stated that the slight strengthening of the SiO bond as a consequence of formation of the hydrogen-bond network produces an increase of ca.  $20\text{--}40\text{ cm}^{-1}$  in the frequency of the  $\nu SiO$  normal mode. We observed two strong bands in the IR spectrum of the liquid phase, at  $826$  and  $841\text{ cm}^{-1}$ , and a broad band centered at  $835\text{ cm}^{-1}$  in the Raman spectrum. The frequency of the stretching of hydrogen-bonded SiO is predicted with the B3LYP/aug-cc-pVDZ method at  $840\text{ cm}^{-1}$ , i.e.,  $32\text{ cm}^{-1}$  shifted from its theoretical value in the case of the monomer I. This value agrees with the experimental observation of one vibrational band at  $841\text{ cm}^{-1}$  in the IR spectrum of the liquid phase. As for the  $826\text{ cm}^{-1}$  band, we think that its presence may be indicative of formation of hydrogen-bonded oligomers of different size, an assumption that may be reinforced by the results reported in refs 4 and 5e dealing with the vibrational spectra of cyclic oligomers of the silanol molecule. In these systems, the  $\nu SiO$  normal modes of the different SiO bonds are predicted to lie within a range of ca.  $40$ ,  $30$ , and  $20\text{ cm}^{-1}$  in the case of the dimer, trimer, and tetramer, respectively. Therefore, the experimental splitting of  $15\text{ cm}^{-1}$  observed for triethylsilanol may be indicative of formation of cyclic H-bonded oligomers of the species.

The next normal mode of the silanol group in this study is the SiOH deformation. In the IR spectrum of the gas phase, this normal mode is assigned to a band appearing at  $855\text{ cm}^{-1}$ .

Nevertheless, this band was not observed in either the IR spectrum of the liquid phase or the Raman spectrum. In the theoretical vibrational spectrum of the model dimer, two modes, with the largest contribution of the SiOH stretching coordinate, are located at  $893$  and  $1077\text{ cm}^{-1}$  (in addition to them, some other modes have a certain contribution of this coordinate). The complex profile of the IR spectrum in this region makes it difficult to identify the first of them in the liquid phase, although a weak band at  $870\text{ cm}^{-1}$  (not assigned to any of the normal modes of the monomer) is observed in the Raman spectrum that may be tentatively assigned to the SiOH deformation of one of the groups involved in the hydrogen bond. The second normal mode with the  $1077\text{ cm}^{-1}$  frequency has a clear correspondence with the band observed in both the Raman and IR spectra of the liquid phase at  $1086\text{ cm}^{-1}$ . Nonetheless, two more bands are observed in that region of the IR spectra of the liquid phase, specifically at  $1121$  and  $1046\text{ cm}^{-1}$ . These bands may be assigned, as in the case of the  $\nu SiO$  mode, to different H-bonded oligomers of the species in the sample. In any case, our proposed assignment is in agreement with the results by Ignatyev et al.<sup>5e</sup> for trimethylsilanol that attributed an observed band at  $1074\text{ cm}^{-1}$  to deformation of the SiOH bond angle in H-bonded oligomers.

Finally, as for the OH bond stretching normal mode we observe three bands in the IR spectrum of the liquid phase: the strong and broad band of the hydrogen-bonded network centered at  $3308\text{ cm}^{-1}$  and two smaller absorption peaks at  $3671$  and  $3700\text{ cm}^{-1}$ . In contrast, only one band was observed in the IR spectrum of the gas phase at  $3730\text{ cm}^{-1}$  assigned to the isolated OH group stretching. The results obtained from the theoretical calculation of the vibrational spectrum of the triethylsilanol dimer state that a slight difference exists between the calculated frequencies for the OH stretching in the monomer,  $3871\text{ cm}^{-1}$ , and the dimer, i.e.,  $3864\text{ cm}^{-1}$ . This difference is sensibly smaller than the experimentally observed red shift that this band suffers in the liquid phase (ca.  $30\text{ cm}^{-1}$ ) but, in addition to the appearance of one more band at  $3671\text{ cm}^{-1}$ , may evidence the existence of isolated H-bonded oligomers of moderate size in the liquid phase.

## Conclusions

(1) It has been demonstrated that 12 different conformers represent minima at the potential-energy surface of the triethylsilanol molecule using the B3LYP and MP2 methods with the 6-31G\* and aug-cc-pVDZ basis sets. Theoretical estimations of the gas-phase populations in terms of Boltzmann's distribution law, applying the calculated  $\Delta G$  values, stated that only five of the stable conformers would be in a percentage higher than 10%.

(2) Within each conformer, the hyperconjugative effects can explain the shortening of the SiC bond in the anti position with respect to the OH bond and the smaller OSiC bond angle in that position, comparing with the other two ethyl groups in the molecule.

(3) The assignment of the complete vibrational spectrum of triethylsilanol has been carried out using experimental data from newly recorded IR (of the liquid and gas phases) and Raman (of the liquid phase) spectra of the species and the theoretical spectra predicted at the B3LYP/6-31G\* level for five main conformers with implementation of the force fields scaling.

(4) Use of the SQMFF methodology allowed us to obtain scale factors for the vibrations of the SiOH group, i.e., 0.961 for the OH stretching normal mode, 0.916 for the SiO stretching normal mode, and 0.914 for the SiOH valence angle normal mode.

(5) The effect of hydrogen bonding on the frequencies of the vibrational bands of the silanol group in the liquid phase have been analyzed using a dimer built from two units of conformer I, optimized at the B3LYP/aug-cc-pVDZ level with the following results: (a) the torsional SiO normal mode suffers a blue shift of ca. 400 cm<sup>-1</sup>, (b) the stretching of the SiO bond is blue shifted by ca. 40 cm<sup>-1</sup> in the spectra of liquid phase with respect to the IR spectrum of the gas phase, and (c) the deformation of the SiOH bond angle appears ca. 200 cm<sup>-1</sup> higher in the liquid phase than in the gas phase.

(6) The presence of oligomers of relatively large size in the liquid phase was proposed. This conclusion is based on the observed shifts of the vibrational bands of the silanol group.

**Acknowledgment.** M. Montejo thanks Fundación Ramón Areces for a Ph.D. studentship supporting this work. The authors thank Francisco Hermoso and Marina Gómez for their help in recording spectra and Tom Sundius for allowing the use of MOLVIB. Financial support from the MEC-FEDER Spanish project (CTQ2006-11306/BQU) and Andalusian Government (FQM-173) is gratefully acknowledged.

**Supporting Information Available:** Cartesian coordinates, molecular representation, IR spectrum. This material is available free of charge via the Internet at <http://pubs.acs.org>.

## References and Notes

- (1) Brinker, C. J.; Scherer, G. W. *Sol-Gel Science: The Physics and Chemistry of Sol-Gel Processing*; Academic Press: San Diego, CA, 1989.
- (2) (a) Santos, J. C.; Reis, M. M.; Machado, R. A. F.; Bolzan, A.; Sayer, C.; Giudici, R.; Araujo, P. H. H. *Ind. Eng. Chem. Res.* **2004**, *43*, 7282. (b) Lee, Y. T.; Jen, H. H. *J. Non-Cryst. Solids* **2004**, *342*, 39. (c) Li, Y. S.; Le, K. *Spectrochim. Acta A* **2004**, *60*, 927. (d) Li, Y. S.; Wright, P. B.; Puritt, R.; Tran, T. *Spectrochim. Acta A* **2004**, *60*, 2759. (e) Sassi, Z.; Bureau, J. C.; Bakkali, A. *Vib. Spectrosc.* **2002**, *28*, 299. (f) Urlaub, R.; Posset, U.; Thull, R. *J. Non-Cryst. Solids* **2000**, *265*, 276. (g) Riegel, B.; Plittersdorf, S.; Kiefer, W.; Hüsing, N.; Schubert, U. *J. Mol. Struct.* **1997**, *410–411*, 157. (h) Afifi, M. S.; Mohamed, T. A. *Al-Azhar Bull. Sci.* **1997**, *8*, 63. (i) Capozzi, C. A.; Pye, L. D.; Condrate, R. A. *Mater. Lett.* **1992**, *15*, 130.
- (3) (a) Raghavachari, K.; Chandrasekhar, J.; Frisch, M. J. *J. Am. Chem. Soc.* **1982**, *104*, 3779. (b) Sauer, J.; Ahlrichs, R. *J. Chem. Phys.* **1990**, *93*, 2575. (c) Hill, J. R.; Sauer, J. *Mol. Phys.* **1991**, *73*, 335. (d) Nicholas, J. B.; Winans, R. E.; Harrison, R. J.; Iton, L. E.; Curtiss, L. A.; Hopfinger, A. J. *J. Phys. Chem.* **1992**, *96*, 10247. (e) Darling, C. L.; Schlegel, H. B. *J. Phys. Chem.* **1993**, *97*, 8207. (f) Stave, M. S.; Nicholas, J. B. *J. Phys. Chem.* **1993**, *97*, 9630. (g) Bleiber, A.; Sauer, J. *Chem. Phys. Lett.* **1995**, *238*, 243. (h) Nicholas, J. B.; Feyereisen, M. *J. Chem. Phys.* **1995**, *103*, 8031. (i) Koput, J. *J. Phys. Chem. A* **2000**, *104*, 10017. (j) Tielens, F.; DeProft, F.; Geerlings, P. *J. Mol. Struct. (Theochem)* **2001**, *542*, 227. (k) Partal, F.; López González, J. J.; Márquez, F. *J. Mol. Spectrosc.* **2005**, *223*, 203.
- (4) Ignatyev, I. S.; Partal, F.; López González, J. J. *J. Phys. Chem. A* **2002**, *106*, 11644.
- (5) (a) Peuker, K.; Lazarev, A. N. *Bull. Acad. Sci. U.S.S.R.* **1968**, *4*, 1716. (b) Rouviere, J.; Tabacik, V.; Fleury, G. *Spectrochim. Acta A* **1973**, *29*, 229. (c) Kriegsmann, H. *Z. Anorg. Allg. Chem.* **1958**, *294*, 113. (d) Bueno, W. A. *Spectrochim. Acta A* **1980**, *36*, 1059. (e) Ignatyev, I. S.; Partal, F.; López González, J. J.; Sundius, T. *Spectrochim. Acta A* **2004**, *60*, 1169.
- (6) (a) Rauhut, G.; Pulay, P. *J. Phys. Chem.* **1995**, *99*, 3093. (b) Fogarasi, G.; Zhou, X.; Taylor, P. W.; Pulay, P. *J. Am. Chem. Soc.* **1992**, *114*, 8191. (c) Fogarasi, G.; Pulay, P. Ab initio calculations of force fields and vibrational spectra. In *Vibrational Spectra and Structure*; Durig, J. R., Ed.; Elsevier: New York, 1985; Vol 14.
- (7) (a) Montejo, M.; Wann, D. A.; Partal, F.; Márquez, F.; Rankin, D. W. H.; López González, J. J. *J. Phys. Chem. A* **2007**, *111*, 2870. (b) Montejo, M.; Hinchley, S. L.; Ben Altabef, A.; Robertson, H. E.; Partal, F.; Rankin, D. W. H.; López González, J. J. *J. Phys. Chem. Chem. Phys.* **2006**, *8*, 477. (c) Montejo, M.; Partal, F.; Márquez, F.; Ignatyev, I. S.; López González, J. J. *Spectrochim. Acta A* **2005**, *62*, 293. (d) Montejo, M.; Partal, F.; Márquez, F.; López González, J. J. *Spectrochim. Acta A* **2005**, *62*, 1058. (e) Montejo, M.; Partal, F.; Márquez, F.; Ignatyev, I. S.; López González, J. J. *J. Mol. Struct.* **2005**, *331*, 744.
- (8) (a) Ryskin, Ya. I.; Voronkov, M. G. *Zhur. Fiz. Khim.* **1956**, *30*, 2275. (b) Ryskin, Ya. I. *Opt. Spektrosk.* **1958**, *4*, 532. (c) Ryskin, Ya. I.; Voronkov, M. G.; Shabarova, Z. I. *Izv. Akad. Nauk SSSR, Ser. Khim.* **1959**, *1019*. (d) Ryskin, Ya. I.; Voronkov, M. G. *Collect. Czech. Chem. Commun.* **1959**, *24*, 3816.
- (9) (a) Licht, K.; Kriegsmann, H. *Z. Anorg. Allg. Chem.* **1963**, *323*, 190. (b) Licht, K.; Kriegsmann, H. *Z. Anorg. Allg. Chem.* **1963**, *323*, 239. (c) Nillius, O.; Kriegsmann, H. *Spectrochim. Acta A* **1970**, *26*, 121.
- (10) Carteret, C. *Spectrochim. Acta A* **2006**, *64*, 670.
- (11) Frisch, M. J.; Trucks, G. W.; Schlegel, H. B.; Scuseria, G. E.; Robb, M. A.; Cheeseman, J. R.; Montgomery, J. A., Jr.; Vreven, T.; Kudin, K. N.; Burant, J. C.; Millam, J. M.; Iyengar, S. S.; Tomasi, J.; Barone, V.; Mennucci, B.; Cossi, M.; Scalmani, G.; Rega, N.; Petersson, G. A.; Nakatsuji, H.; Hada, M.; Ehara, M.; Toyota, K.; Fukuda, R.; Hasegawa, J.; Ishida, M.; Nakajima, T.; Honda, Y.; Kitao, O.; Nakai, H.; Klene, M.; Li, X.; Knox, J. E.; Hratchian, H. P.; Cross, J. B.; Bakken, V.; Adamo, C.; Jaramillo, J.; Gomperts, R.; Stratmann, R. E.; Yazyev, O.; Austin, A. J.; Cammi, R.; Pomelli, C.; Ochterski, J. W.; Ayala, P. Y.; Morokuma, K.; Voth, G. A.; Salvador, P.; Dannenberg, J. J.; Zakrzewski, V. G.; Dapprich, S.; Daniels, A. D.; Strain, M. C.; Farkas, O.; Malick, D. K.; Rabuck, A. D.; Raghavachari, K.; Foresman, J. B.; Ortiz, J. V.; Cui, Q.; Baboul, A. G.; Clifford, S.; Cioslowski, J.; Stefanov, B. B.; Liu, G.; Liashenko, A.; Piskorz, P.; Komaromi, I.; Martin, R. L.; Fox, D. J.; Keith, T.; Al-Laham, M. A.; Peng, C. Y.; Nanayakkara, A.; Challacombe, M.; Gill, P. M. W.; Johnson, B.; Chen, W.; Wong, M. W.; Gonzalez, C.; Pople, J. A. *Gaussian 03*, Revision C.01; Gaussian, Inc.: Wallingford, CT, 2004.
- (12) (a) Sundius, T. *J. Mol. Struct.* **1990**, *218*, 321. (b) Sundius, T. *Vib. Spectrosc.* **2002**, *29*, 89.
- (13) Reed, A. E.; Curtiss, L. A.; Weinhold, F. *Chem. Rev.* **1988**, *88*, 899.
- (14) Glendening, E. D.; Reed, A. E.; Carpenter, J. E.; Weinhold, F. *NBO*, v. 3.1; Madison, WI, 1988.